

Letter pubs.acs.org/NanoLett

Phenylacetylene-Terminated Poly(Ethylene Glycol) as Ligands for Colloidal Noble Metal Nanoparticles: a New Tool for "Grafting to" **Approach**

Hanyi Duan, Tiangang Yang, William Sklyar, Belinda Chen, Yuliang Chen, Lindsey A. Hanson, Shouheng Sun, Yao Lin, and Jie He*



Cite This: Nano Lett. 2024, 24, 5847-5854



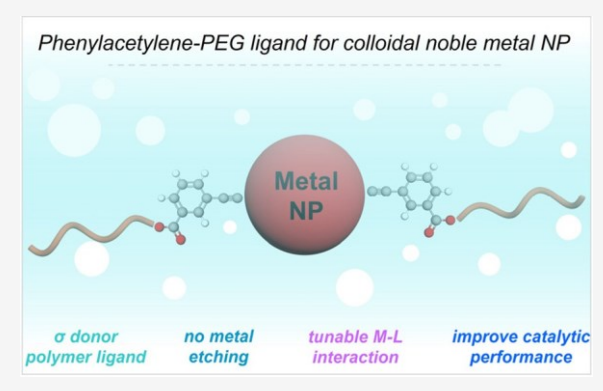
ACCES\$

III Metrics & More

Article Recommendations

Supporting Information

ABSTRACT: We report a new design of polymer phenylacetylene (PA) ligands and the ligand exchange methodology for colloidal noble metal nanoparticles (NPs). PA-terminated poly(ethylene glycol) (PEG) can bind to metal NPs through acetylide (M-C&C-R) that affords a high grafting density. The ligand–metal interaction can be switched between σ bonding and extended π backbonding by changing grafting conditions. The σ bonding of PEG-PA with NPs is strong and it can compete with other capping ligands including thiols, while the π backbonding is much weaker. The σ bonding is also demonstrated to improve the catalytic performance of Pd for ethanol oxidation and prevent surface absorption of the reaction intermediates. Those unique binding characteristics will enrich the toolbox in the control of colloidal surface chemistry and their applications using polymer ligands.



KEYWORDS: phenylacetylene, metal nanoparticles, polymer ligand, sigma donor, surface chemistry

urface ligands play a key role in controlling not only the Jolloidal stability of metal nanoparticles (NPs) but also how NP cores function and/or interact with molecules and surroundings.^{1,2} Adding polymer ligands to NPs, termed polymer grafted nanoparticles (PGNPs), is of particular interest, given the rich chemistry of polymers to design and tailor the surface properties of metal NPs.³⁻⁹ Among many examples, poly(ethylene glycol) (PEG) grafted plasmonic NPs, e.g., gold NPs (AuNPs), have received tremendous interest due to their biocompatibility and antifouling properties for applications like bioimaging and theranostics. 10-13 In the "grafting to" approach, polymer ligands can replace the original capping ligands on presynthesized NPs while not changing their well-defined nanostructures. 14-18 Thiol-terminated polymers have been extensively used in the modification of various metal NPs through the formation of metal-thiolate binding as the self-assembled monolayers. 14,19-24 In regard to AuNPs, Au-thiolate (Au-S) has a moderate binding energy of 126 kJ/ mol as a semicovalent bond, 25,26 although it becomes dynamic at elevated temperatures.^{27–29} Other metal-organic bindings, such as N-heterocyclic carbenes (NHCs), have recently risen as promising alternatives to thiols due to the chemical stability of metal-C bonds against oxidants and heating.^{30–36} NHCs interact with AuNPs via Au-C binding with a binding energy of 158 kJ/mol.³⁷ As a strong σ donor, NHCs have proven to be efficient in stabilizing NPs and tuning their selectivity in various catalytic reactions, e.g., hydrogenation and CO₂

electroreduction.³⁸⁻⁴⁰ More recent reports have shown that strong metal-C bonds are even stronger than metal-metal interaction. 41,42 As such, surface etching or dissolution of metal NPs has been troublesome where nanostructures of metal NPs were disrupted.⁴³ Thus, it is highly desirable to design ligands as a weaker σ donor compared with NHCs but possessing strong metal—C binding with a variety of NPs.

Acetylides (M-C&C-R) generated between terminal alkynes and transition metals represent another strong metal-C. In syntheses of metal nanoclusters, phenylacetylene (PA) derivatives have been extensively used as capping ligands. 44,45 Due to its unique conjugation, PA-based ligands are known to bind with metals through both σ bonding (as an σ donor) and π backbonding (as a π acceptor).^{46–48} Despite their success on nanoclusters, PA-containing polymer ligands have not yet been reported. In this Letter, we report a PAcontaining PEG (PEG-PA) ligand as a versatile ligand to functionalize metal NPs (Figure 1a). PEG-PA could be easily prepared on a large scale through one step esterification. The

Received: March 6, 2024 April 19, 2024 Revised: Accepted: April 30, 2024 Published: May 3, 2024





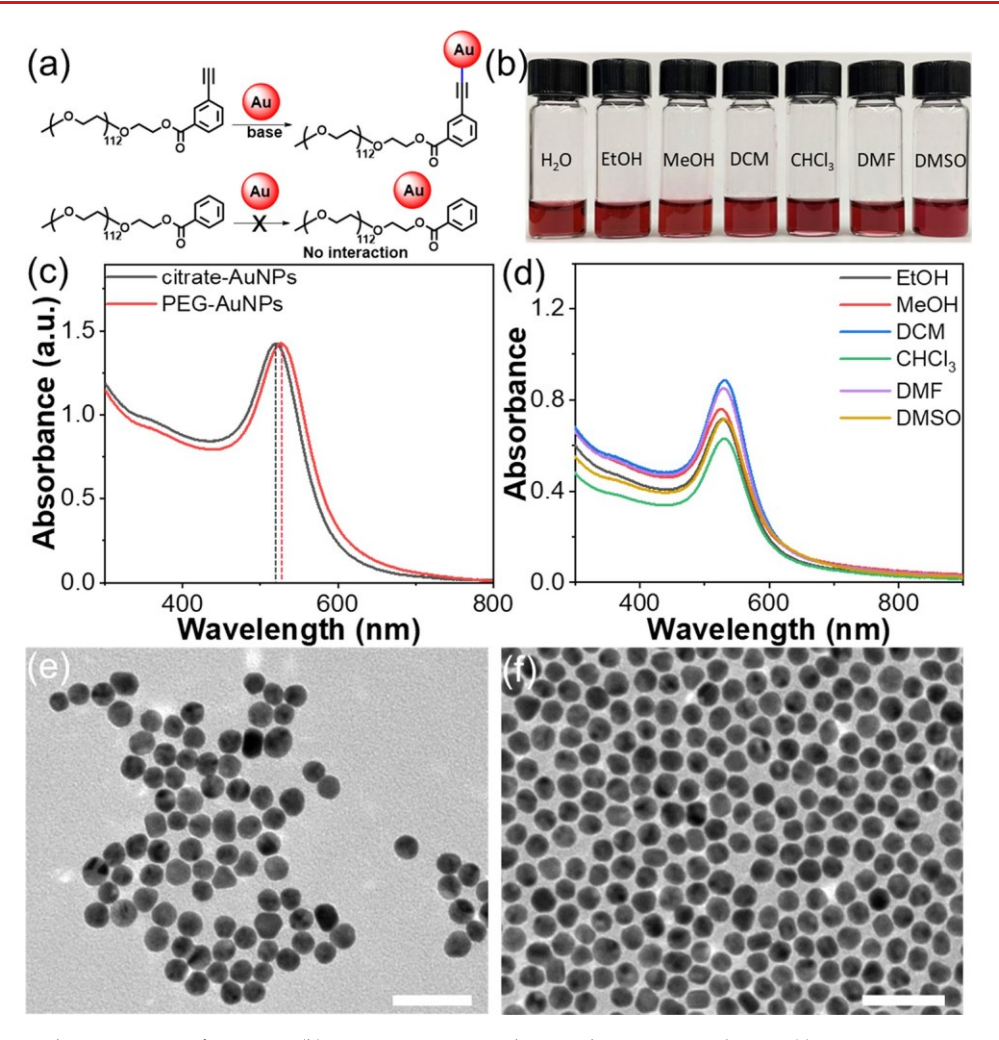


Figure 1. (a) PEG-PA or benzoate to graft AuNPs. (b) PEG-PA-AuNPs dispersed in various solvents. (c) UV-vis spectrum of AuNPs in water before and after PEG modification. (d) UV-vis spectra of PEG-PA-AuNPs dispersed in various solvents. (e,f) TEM images of AuNPs before (e) and after (f) PEGylation (scale bar = 50 nm).

ligand—metal interaction can be altered by the ligand exchange conditions. Under basic conditions, PEG–PA preferentially bound metal NPs through σ bonding; while under neutral conditions, PEG–PA favored binding with metal NPs through extended π backbonding. The π backbonding had a weak binding strength, while the σ bonding of PEG–PA could effectively modify NPs with different sizes, compositions, and surface capping agents including thiol-terminated polymers.

PEG-PA was synthesized by esterification using monomethyl ether PEG (MW 5000 g/mol) and 3-ethynylbenzoic acid (see details in the SI). The final chemical structure was confirmed by ¹H NMR (Figure S1). PEG-PA was used to modify citrate-capped AuNPs (13.5 \pm 1.2 nm, Figure S2). Typically, concentrated AuNPs were added to a PEG-PA aqueous solution (2 mg/mL). The solution pH was adjusted to ca. 12 with 1 M NaOH. The mixture was then heated at 60 °C for 2 h. The final AuNPs were purified by four centrifugation cycles in water to remove unbound PEG-PA as much as possible. Purified AuNPs could be readily dispersed in any good solvents for PEG. Figure 1b shows the image of AuNPs dispersed in water and various organic solvents, all of which displayed a red color due to the local surface plasmon resonance (LSPR) of AuNPs. Figure 1c shows the UV – vis absorption spectroscopy of AuNPs capped with citrate and PEG-PA. In water, a 7 nm red-shift of the LSPR peak was

seen. The LSPR peaks of AuNPs have also been clearly seen in different organic solvents (Figure 1d). Those results confirm the good colloidal stability after PEGylation. Our control experiments showed that PEG ending with a hydroxyl (–OH) group or benzoate cannot stabilize AuNPs (Figure S3), which ruled out the possibility of a PEG main chain and aromatic ring interacting with AuNPs. Also, the isomers of PA did not play a significant role in ligand grafting, as PEG with all *o-, m-,* and *p*-ethynylbenzoates could modify AuNPs similarly (Figure S4). The morphology of AuNPs before and after modification was examined by transmission electron microscopy (TEM) as shown in Figure 1e,f. After PEGylation, AuNPs remained spherical with no aggregation or a change in size (Figure S2) after purification.

Figure 2a shows the ¹H NMR spectra of free PEG and PEG-PA-AuNPs after purification. A singlet peak at 3.59 ppm (-CH₂-CH₂-O-) was found for PEG-PA-AuNPs, close to that of the free PEG backbone at 3.63 ppm. There was a clear peak broadening due to the limited chain mobility of PEG after grafting to AuNPs. The peak shift of the aromatic protons was more pronounced (Figure 2b). For PEG-PA, all four protons are well-resolved, and the four peaks shifted to a much broader range after grafting on AuNPs. PEG-grafted AuNPs had one set of aromatic protons, suggesting an exclusive binding of PEG on AuNPs. To confirm such

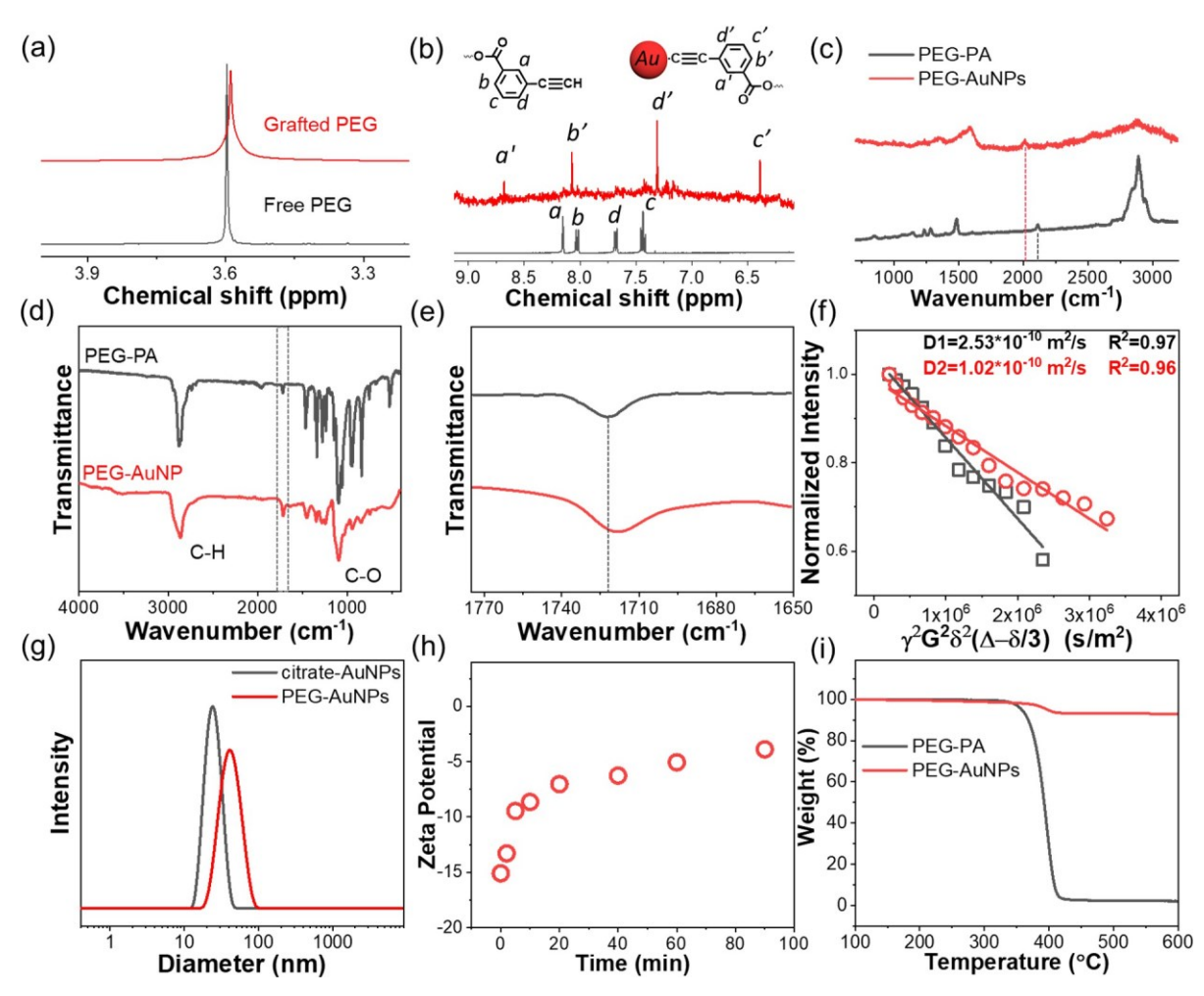


Figure 2. (a−g) ¹H NMR, Raman/FTIR spectra, DOSY attenuation plot, DLS of free PEG−PA (black) and PEG−PA−AuNPs (red; a, CDCl₃ as solvent; b, CD₂Cl₂ was used to avoid the interference of residual solvent peak). (e) Zoom-in spectra of C�O stretching of PEG−PA (black) and PEG−PA−AuNPs (red). (h) Plotting zeta potential of AuNPs against ligand exchange time. (i) TGA curves of PEG−PA (black) and PEG−PA−AuNPs (red).

transformation, surface enhanced Raman spectroscopy (SERS) was employed to monitor the change of C&C stretching by taking advantage of the plasmonic field of AuNPs. Figure 3c shows that the C&C of unbound PEG-PA appeared at 2110 cm⁻¹. For PEG-AuNPs, the peak shifted to 2018 cm⁻¹. Since the formation of acetylide binding (Au–C Φ C) through σ interaction would weaken the C&C triple bond, the red-shift of ~90 cm⁻¹ is indicative of the polymer grafting through acetylide binding. This peak shift is also close to those values reported in the acetylide binding of molecular Au complexes and clusters. 48,49 The FT-IR spectra in Figure 2d also display the vibrational feature of PEG. Strong C-H and C-O stretching peaks can be identified at 2868 and 1093 cm⁻¹, respectively. Compared to free PEG, the COO stretching peak in ester for PEG-AuNPs shifted from 1721 to 1718 cm⁻¹ (Figure 2e), presumably due to the formation of acetylide.

We used diffusion ordered spectroscopy (DOSY) to probe the diffusion coefficient (D) of unbound and grafted PEG–PA to confirm the surface grafting of PEG on the AuNPs. Through linear fitting of the DOSY attenuation (Figure 2f), the D of unbound and grafted PEG–PA was extracted to be 2.53×10^{-10} and 1.02×10^{-10} m²/s, respectively, using the methylene peak at 3.6 ppm. A lower D further suggested a slower diffusion for grafted PEG due to surface confinement. The hydro-

dynamic radius (R_h) is estimated to be 2.1 and 5.2 nm for unbound PEG-PA and PEG-PA-AuNPs, respectively (see SI for details). Dynamic light scattering (DLS) was used to confirm the R_h (Figure 2g). For unmodified citrate-AuNPs, R_h was ~11 nm, slightly larger than the radius of AuNPs measured from TEM owing to their ionic citrate shell. The R_h increased to ~19 nm for the PEG-PA-AuNPs. The difference between R_h of PEG-AuNPs and the radius of the Au core (r) was much greater than the end-to-end distance of globular PEG, indicating the PEG chain stretching ratio of ~1.8 times (see the SI). It should be noted that the difference of R_h between DLS and DOSY measurements is from the average methods from DOSY and DLS, consistent with other polymer-grafted NPs reported recently.⁵⁰

The binding kinetics of PEG-PA were monitored by the change in zeta potential of AuNPs. As citrate-capped AuNPs were negatively charged, ligand replacement by PEG-PA would result in the loss of negatively charged citrate. Figure 2h plots the change in zeta potential as a function of ligand exchange time. The negative charge of AuNPs decreased and plateaued within 20 min, suggesting fast ligand replacement of citrate by PEG-PA. The ligand exchange kinetics are comparable to thiol-terminated PEG (PEG-SH; Figure S5). With extended incubation to 1 h, the zeta potential of AuNPs

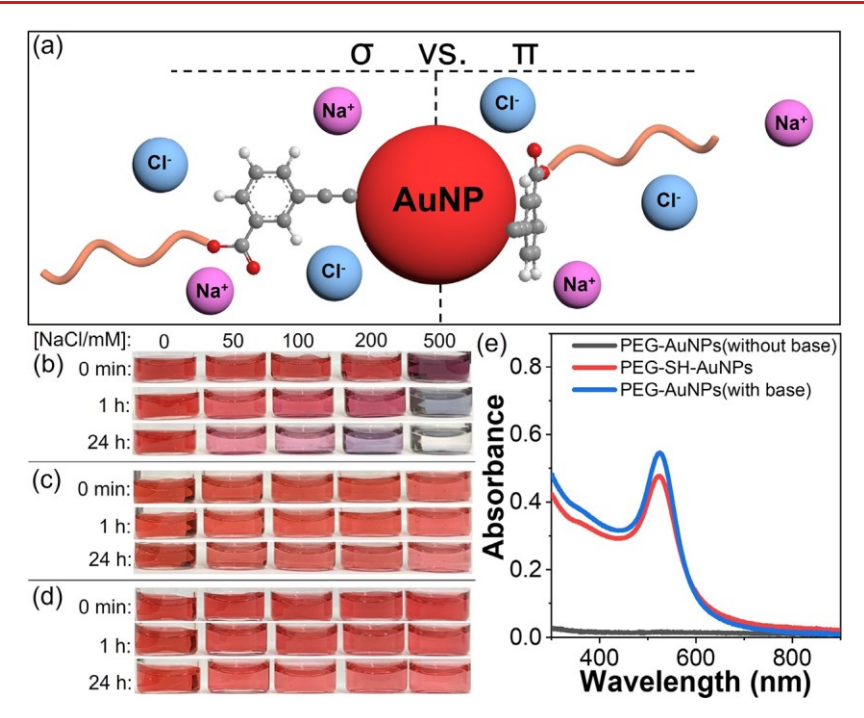


Figure 3. Colloidal stability of PEG grafted AuNPs against NaCl: (a) scheme showing AuNPs grafted by PEG-PA through σ and π interaction; (b) PEG-PA-AuNPs modified without a base; (c) PEG-SH-AuNPs; (d) PEG-PA-AuNPs modified with a base. (e) UV-vis spectra of PEG-grafted AuNPs at 500 mM NaCl after 24 h.

grafted with PEG-PA reached -5 mV, suggesting the high surface coverage of PEG-PA to yield nearly neutral AuNPs. The grafting density of PEG-PA was further determined by thermogravimetric analysis (TGA) to be 0.27 chains/nm² (see the calculation details in the SI, Figure 2i). Those results suggest dense polymer brushes formed on the surface of AuNPs comparable to thiol-terminated PEG (0.1–0.5 chains/nm²). 51,52

Interestingly, the grafting of PEG-PA to AuNPs could take place without a base, contradictory to the acetylide binding model. After incubating AuNPs with PEG-PA without a base, we confirmed the surface grafting using TGA where the grafting density of PEG-PA was as high as 0.37 chains/nm² (Figure S6). In the absence of a base, PEG-AuNPs, however, exhibited different NMR (Figure S7)46 and Raman (Figure S8) features, although the diffusion coefficient of PEG is similar to that of PEG-PA-Au with a base (Figure S7b). We speculated that PEG-PA interacted with AuNPs through extended π backbonding of phenylacetylene, much less common but reported previously in simulation.⁵³ The π backbonding can occur in a flat geometry where the two C atoms in $H-C\phi C-$ PA-PEG bind with two Au atoms atop the nearest Au sites. The two different binding modes of PEG-PA show different stabilities to AuNPs. We studied the colloidal stability of PEGylated AuNPs against the electrolyte. Figure 3b and d show the pictures of AuNPs modified with PEG-PA with and without a base in the presence of NaCl at various concentrations. AuNPs modified with PEG-SH were used as a control (Figure 3c). PEG-PA-AuNPs prepared without a base started to aggregate immediately with 500 mM of NaCl. After 1 h, it also became unstable at 100 and 200 mM NaCl. However, for AuNPs grafted by PEG-SH and PEG-PA in the presence of a base, there is no color change, as shown in Figure 3c,d. The reddish color of the AuNPs was preserved with various concentrations of NaCl, also confirmed by UV-vis

(Figure 3e). Those results indicate that, as a π acceptor, PEG–PA is much weaker, but as a σ donor, PEG–PA can stabilize AuNPs against electrolytes. We also tested their colloidal stability under an oxidative environment. AuNPs modified by PEG–PA through σ bonding had better stability against H₂O₂ (50–500 mM) than PEG–SH (Figure S9).

The σ bonding is strong, and it can replace SH through ligand exchange. With AuNPs grafted by thiol-terminated polystyrene (PS, M_n = 17 kDa, D = 1.2), we demonstrated a simple phase transfer experiment using PEG-PA (Figure 4). PS-grafted AuNPs are hydrophobic. In a mixture of toluene and water, they favored dispersion in toluene. After ligand exchange with PEG-PA in the presence of triethylamine (TEA) for 2 h, a clear emulsion was seen as amphiphilic AuNPs with mixed PS and PEG ligands stabilizing oil-in-water emulsion. After ligand exchange for 12 h, AuNPs completely transferred to water, suggesting that thiol-terminated PS was replaced by PEG-PA and that the surface became hydrophilic. Such ligand replacement did not occur without TEA. On the other hand, similar ligand replacement of PEG-PA by thiolterminated PS did not transfer AuNPs from water to toluene (Figure S10).

Furthermore, PEG-PA can modify various NPs with different compositions, sizes, and surface capping agents. Citrate-capped Au seeds (3.5 nm) could be modified through a phase transfer method at the interface of water and dichloromethane (DCM). By dissolving PEG-PA and triethylamine (TEA) in DCM, citrate-capped Au seeds could be transferred from water to DCM within 10 min under stirring (Figure S11). Other weak bases, *e.g.*, *tert*-butylamine, also work for the interfacial transfer, and the basicity does not seem to be critical for the ligand exchange rate. Oleylamine-capped AuNPs with a similar size could be modified using PEG-PA with TEA directly in chloroform. Modified AuNPs could be redispersed into polar solvents including water that

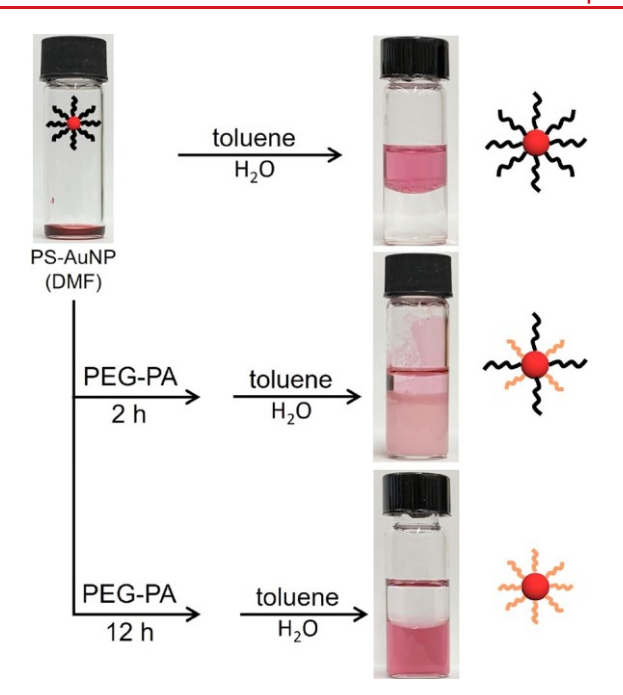


Figure 4. Ligand exchange of AuNPs grafted with PS-SH by PEG-PA using phase transfer.

are not compatible with their capping agent (Figure S12). A similar strategy was successfully applied to platinum (Pt) or palladium (Pd) NPs capped with oleylamine (Figure S13). This nonpolar–polar solubility transition for AuNPs together with UV–vis data provides solid evidence for PEG–PA grafting (Figure S14).

PEG-PA as a strong σ donor can also be used to improve the catalytic performance of metal NPs. Using Pd nanoclusters

supported on nitrided carbon (Pd/C) as an example, 54,55 Figure 5a,b show the TEM images of Pd/C before and after modification with PEG-PA in the presence of TEA. The diameter of Pd/C after modification was nearly identical to that prior to surface grafting (Figure 5c). No etching of PdNPs was seen, while polymer NHCs would strongly etch those small Pd nanoclusters (Figure S15). We measured the electrochemical active surface area (ECSA) of Pd/C. The surface area decreased from 0.68 \pm 0.1 for Pd/C to 0.26 \pm $0.05 \text{ cm}^2/\mu\text{g}$ for PEG-PA-Pd (Figure 5d). As a control, Pd with PEG-SH has an ECSA of 0.48 ± 0.07 cm²/ μ g. The smaller ECSA with PEG-PA is attributed to the surface crowdedness of grafted PEG chains that block the ion exchange onto PdNPs, as reported previously.³⁹ Note that the reduction peak for oxygenated Pd has a ~90 mV (vs saturated calomel electrode) positive shift compared to unmodified and PEG-SH modified Pd, indicating its electron-rich surface enabled by the σ donation of PEG-PA. CO stripping voltammetry was used to study the surface Pd electronic state. The CO oxidation peak on PEG-PA-Pd was at 0.94 V, about 100 mV more positive than that on Pd/C (0.84 V). The shift of the CO oxidation peak is attributed to the electron-rich Pd surface arising from the σ donating of acetylide, comparable to that of NHCs.38 The catalytic activity for ethanol electrooxidation was tested by using 0.6 M ethanol at pH 13. Figure 5f shows the cyclic voltammograms (CVs) for ethanol electro-oxidation. Both Pd/C and PEG-PA-Pd showed very similar catalytic activity, suggesting that grafted PEG-PA does preserve the intrinsic activity of Pd. For pristine Pd/C, a common large backward oxidation peak was seen at -0.39 V with a forward to backward current density (J_f/J_b) ratio of 1.2 for Pd. This backward oxidation peak is often assigned to the absorbed intermediate species on PdNPs.⁵⁶ With PEG-SH, the activity of PdNPs (J_f) decreased about

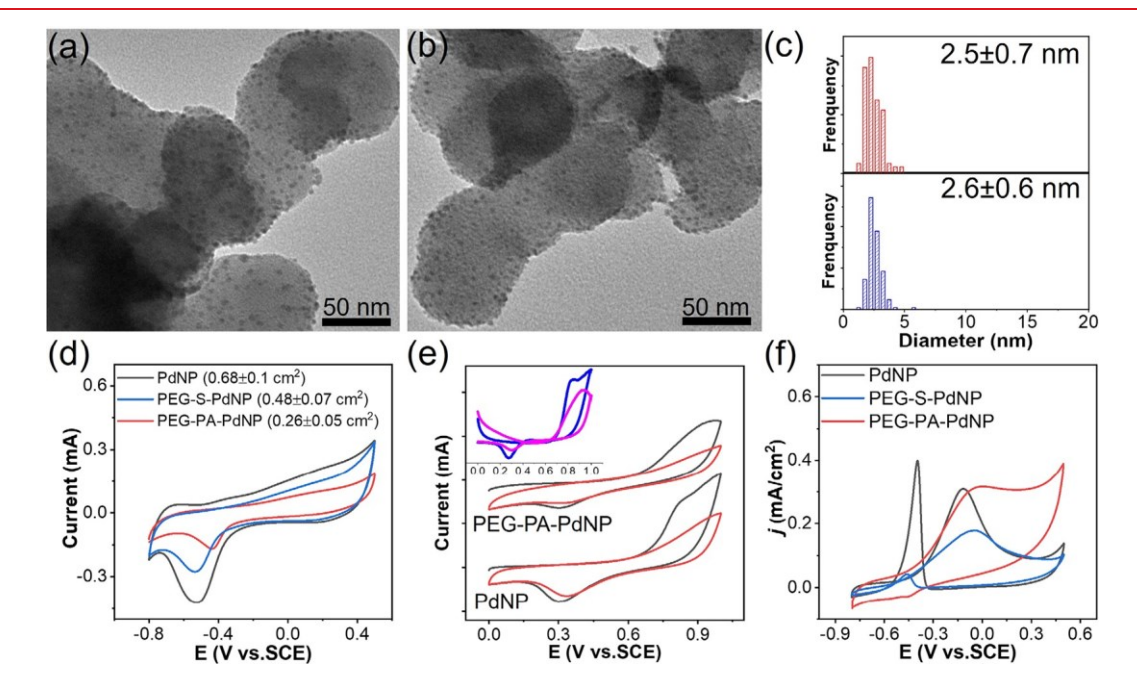


Figure 5. (a–d) TEM images and size distribution of Pd/C before (a, c top) and after (b, c bottom) surface grafting. (d) CVs to determine ECSA of Pd/C (black), PEG-S-Pd/C (blue) and PEG-PA-Pd/C (red) in N_2 saturated 0.1 M KOH at 0.5 V/s. (e) CO stripping voltammetry (black, first cycle; red, second cycle) for Pd/C (upper) and PEG-PA-Pd/C (lower). The inset shows the real CO oxidation peak after background subtraction for PdNPs (blue curve) and PEG-PdNPs (magenta curve). (f) CVs for Pd/C (black), PEG-S-Pd/C (blue) and PEG-PA-Pd/C (red) at 0.05 V/s in N_2 saturated 0.1 M KOH containing 0.6 M ethanol.

50%, although the modified PdNPs exhibited a lower backward absorption with a $J_{\rm f}/J_{\rm b}$ value of 0.23. In contrast, the disappearance of the backward oxidation peak ($J_{\rm b}$) was seen for Pd/C with PEG–PA, without compromising the intrinsic activity of PdNPs. These results suggest that the acetylide motif could prevent catalyst poisoning from reaction intermediates.

In summary, we designed a phenylacetylene-containing polymer ligand for "grafting to" colloidal NPs. PEG-PA, synthesized from a facile esterification reaction, was able to bind to metal NPs through σ or π bonding. In presence of a base, PEG-PA was efficient to modify colloidal AuNPs with a high grafting density of 0.27 chain/nm² within 2 h. PEG-PA could bind with NPs through extended π back-donation in the absence of base. The σ bonding of PEG-PA was strong to modify metal NPs by replacing capping agents, including polymer thiol. We demonstrated the use of one-phase ligand replacement or biphasic phase transfer of metal NPs in the presence of inorganic or organic bases. This new binding motif offers unique advantages in terms of their synthetic capacity to a number of polymers, e.g., polyesters, polyethers, and polyamides, where other binding motifs are less accessible through postpolymerization syntheses.

ASS

ASSOCIATED CONTENT

Supporting Information

The Supporting Information is available free of charge at https://pubs.acs.org/doi/10.1021/acs.nanolett.4c01127.

Synthesis of polymer ligand and nanoparticles; grafting density and stretching ratio calculation; colloidal stability test and electrochemical test details; more NMR, TEM, and RAMAN spectra (PDF)

AUTHOR INFORMATION

Corresponding Author

Jie He − Polymer Program, Institute of Materials Science and Department of Chemistry, University of Connecticut, Storrs, Connecticut 06269, United States; orcid.org/0000-0003-0252-3094; Email: jie.he@uconn.edu

Authors

Hanyi Duan − Polymer Program, Institute of Materials Science, University of Connecticut, Storrs, Connecticut 06269, United States; orcid.org/0000-0001-8720-2761 Tiangang Yang − Department of Chemistry, University of

Connecticut, Storrs, Connecticut 06269, United States
William Sklyar — Department of Chemistry, University of
Connecticut, Storrs, Connecticut 06269, United States
Belinda Chen — Department of Chemistry, University of
Connecticut, Storrs, Connecticut 06269, United States

Yuliang Chen – Department of Chemistry, Brown University, Providence, Rhode Island 02912, United States

Lindsey A. Hanson — Department of Chemistry, Trinity College, Hartford, Connecticut 06106, United States; orcid.org/0000-0002-0226-6115

Shouheng Sun – Department of Chemistry, Brown University, Providence, Rhode Island 02912, United States

Yao Lin − Polymer Program, Institute of Materials Science and Department of Chemistry, University of Connecticut, Storrs, Connecticut 06269, United States; orcid.org/0000-0001-5227-2663

Complete contact information is available at:

https://pubs.acs.org/10.1021/acs.nanolett.4c01127

Author Contributions

J.H. conceived the idea. H.D. performed experiments and collected the data. T.Y. did the electrochemical measurement. W.S. and B.C. contributed to the sample preparation and purification. Y.C. and S.S. provided the Pt and Pd NPs. L.H. provided help on the DOSY experiment. J.H. and Y.L. supervised the project. The manuscript was written through contributions of all authors.

Notes

The authors declare no competing financial interest.

ACKNOWLEDGMENTS

J.H. is grateful for the financial support from the National Science Foundation (CHE 2102245). The TEM images were obtained at the Biosciences Electron Microscopy Facility at the University of Connecticut. This work was also partially supported by the Green Emulsions Micelles and Surfactants (GEMS) Center of the University of Connecticut.

REFERENCES

- (1) Heuer-Jungemann, A.; Feliu, N.; Bakaimi, I.; Hamaly, M.; Alkilany, A.; Chakraborty, I.; Masood, A.; Casula, M. F.; Kostopoulou, A.; Oh, E.; Susumu, K.; Stewart, M. H.; Medintz, I. L.; Stratakis, E.; Parak, W. J.; Kanaras, A. G. The Role of Ligands in the Chemical Synthesis and Applications of Inorganic Nanoparticles. *Chem. Rev.* 2019, 119, 4819—4880.
- (2) Ling, D.; Hackett, M. J.; Hyeon, T. Surface ligands in synthesis, modification, assembly and biomedical applications of nanoparticles. *Nano Today* 2014, *9*, 457–477.
- (3) Zhang, N.-N.; Shen, X.; Liu, K.; Nie, Z.; Kumacheva, E. Polymer-Tethered Nanoparticles: From Surface Engineering to Directional Self-Assembly. *Acc. Chem. Res.* 2022, *55*, 1503–1513.
- (4) Yi, C.; Yang, Y.; Liu, B.; He, J.; Nie, Z. Polymer-guided assembly of inorganic nanoparticles. *Chem. Soc. Rev.* 2020, 49, 465–508.
- (5) Duan, H.; Yang, Y.; Zhang, Y.; Yi, C.; Nie, Z.; He, J. What is next in polymer-grafted plasmonic nanoparticles? *Giant* 2020, 4, No. 100033.
- (6) Pang, X.; He, Y.; Jung, J.; Lin, Z. 1D nanocrystals with precisely controlled dimensions, compositions, and architectures. *Science* 2016, 353, 1268–1272.
- (7) Chen, Y.; Wang, Z.; He, Y.; Yoon, Y. J.; Jung, J.; Zhang, G.; Lin, Z. Light-enabled reversible self-assembly and tunable optical properties of stable hairy nanoparticles. *Proc. Natl. Acad. Sci. U.S.A.* 2018, 115, E1391—E1400.
- (8) Grzelczak, M.; Liz-Marzán, L. M.; Klajn, R. Stimuli-responsive self-assembly of nanoparticles. *Chem. Soc. Rev.* 2019, 48, 1342–1361.
- (9) Liu, Y.; Wang, J.; Zhang, M.; Li, H.; Lin, Z. Polymer-Ligated Nanocrystals Enabled by Nonlinear Block Copolymer Nanoreactors: Synthesis, Properties, and Applications. *ACS Nano* 2020, *14*, 12491–12521.
- (10) Dykman, L.; Khlebtsov, N. Gold nanoparticles in biomedical applications: recent advances and perspectives. *Chem. Soc. Rev.* 2012, *41*, 2256–2282.
- (11) Yang, X.; Yang, M.; Pang, B.; Vara, M.; Xia, Y. Gold nanomaterials at work in biomedicine. *Chem. Rev.* 2015, *115*, 10410–10488.
- (12) Rosi, N. L.; Mirkin, C. A. Nanostructures in Biodiagnostics. *Chem. Rev.* 2005, *105*, 1547–1562.
- (13) Zhang, X.-D.; Wu, D.; Shen, X.; Chen, J.; Sun, Y.-M.; Liu, P.-X.; Liang, X.-J. Size-dependent radiosensitization of PEG-coated gold nanoparticles for cancer radiation therapy. *Biomaterials* 2012, *33*, 6408–6419.

- (14) Nie, Z.; Fava, D.; Kumacheva, E.; Zou, S.; Walker, G. C.; Rubinstein, M. Self-assembly of metal—polymer analogues of amphiphilic triblock copolymers. *Nat. Mater.* 2007, *6*, 609–614.
- (15) He, J.; Liu, Y.; Babu, T.; Wei, Z.; Nie, Z. Self-Assembly of Inorganic Nanoparticle Vesicles and Tubules Driven by Tethered Linear Block Copolymers. *J. Am. Chem. Soc.* 2012, *134*, 11342–11345.
- (16) Liu, K.; Nie, Z.; Zhao, N.; Li, W.; Rubinstein, M.; Kumacheva, E. Step-growth polymerization of inorganic nanoparticles. *Science* 2010, 329, 197–200.
- (17) Hinman, J. G.; Eller, J. R.; Lin, W.; Li, J.; Li, J.; Murphy, C. J. Oxidation State of Capping Agent Affects Spatial Reactivity on Gold Nanorods. *J. Am. Chem. Soc.* 2017, *139*, 9851–9854.
- (18) Liu, Y.; Klement, M.; Wang, Y.; Zhong, Y.; Zhu, B.; Chen, J.; Engel, M.; Ye, X. Macromolecular Ligand Engineering for Programmable Nanoprism Assembly. *J. Am. Chem. Soc.* 2021, *143*, 16163—16172.
- (19) He, J.; Huang, X.; Li, Y.-C.; Liu, Y.; Babu, T.; Aronova, M. A.; Wang, S.; Lu, Z.; Chen, X.; Nie, Z. Self-Assembly of Amphiphilic Plasmonic Micelle-Like Nanoparticles in Selective Solvents. *J. Am. Chem. Soc.* 2013, *135*, 7974–7984.
- (20) Jones, M. R.; Macfarlane, R. J.; Lee, B.; Zhang, J.; Young, K. L.; Senesi, A. J.; Mirkin, C. A. DNA-nanoparticle superlattices formed from anisotropic building blocks. *Nat. Mater.* 2010, *9*, 913–917.
- (21) Sánchez-Iglesias, A.; Grzelczak, M.; Altantzis, T.; Goris, B.; Pérez-Juste, J.; Bals, S.; Van Tendeloo, G.; Donaldson, S. H.; Chmelka, B. F.; Israelachvili, J. N.; Liz-Marzán, L. M. Hydrophobic Interactions Modulate Self-Assembly of Nanoparticles. *ACS Nano* 2012, 6, 11059–11065.
- (22) Grzelczak, M.; Sánchez-Iglesias, A.; Mezerji, H. H.; Bals, S.; Pérez-Juste, J.; Liz-Marzán, L. M. Steric Hindrance Induces crosslike Self-Assembly of Gold Nanodumbbells. *Nano Lett.* 2012, *12*, 4380–4384.
- (23) Kang, J.; Wang, Y.-X.; Peng, F.; Zhang, N.-N.; Xue, Y.; Yang, Y.; Kumacheva, E.; Liu, K. Oxidative Elimination and Reductive Addition of Thiol-Terminated Polymer Ligands to Metal Nanoparticles. *Angew. Chem., Int. Ed.* 2022, *61*, No. e202202405.
- (24) Pan, S.; He, L.; Peng, J.; Qiu, F.; Lin, Z. Chemical-Bonding-Directed Hierarchical Assembly of Nanoribbon-Shaped Nanocomposites of Gold Nanorods and Poly (3-hexylthiophene). *Angew. Chem., Int. Ed.* 2016, *128*, 8828–8832.
- (25) Engel, S.; Fritz, E.-C.; Ravoo, B. J. New trends in the functionalization of metallic gold: from organosulfur ligands to N-heterocyclic carbenes. *Chem. Soc. Rev.* 2017, 46, 2057–2075.
- (26) Lavrich, D. J.; Wetterer, S. M.; Bernasek, S. L.; Scoles, G. Physisorption and Chemisorption of Alkanethiols and Alkyl Sulfides on Au(111). *J. Phys. Chem. B* 1998, *102*, 3456–3465.
- (27) Lee, M.-T.; Hsueh, C.-C.; Freund, M. S.; Ferguson, G. S. Air Oxidation of Self-Assembled Monolayers on Polycrystalline Gold: The Role of the Gold Substrate. *Langmuir* 1998, *14*, 6419–6423.
- (28) Bhatt, N.; Huang, P.-J. J.; Dave, N.; Liu, J. Dissociation and Degradation of Thiol-Modified DNA on Gold Nanoparticles in Aqueous and Organic Solvents. *Langmuir* 2011, *27*, 6132–6137.
- (29) Duan, H.; Luo, Q.; Wei, Z.; Lin, Y.; He, J. Symmetry-Broken Patches on Gold Nanoparticles through Deficient Ligand Exchange. *ACS Macro Lett.* 2021, *10*, 786–790.
- (30) Crudden, C. M.; Horton, J. H.; Ebralidze, I. I.; Zenkina, O. V.; McLean, A. B.; Drevniok, B.; She, Z.; Kraatz, H.-B.; Mosey, N. J.; Seki, T.; Keske, E. C.; Leake, J. D.; Rousina-Webb, A.; Wu, G. Ultra stable self-assembled monolayers of N-heterocyclic carbenes on gold. *Nat. Chem.* 2014, *6*, 409–414.
- (31) Man, R. W. Y.; Li, C.-H.; MacLean, M. W. A.; Zenkina, O. V.; Zamora, M. T.; Saunders, L. N.; Rousina-Webb, A.; Nambo, M.; Crudden, C. M. Ultrastable Gold Nanoparticles Modified by Bidentate N-Heterocyclic Carbene Ligands. *J. Am. Chem. Soc.* 2018, 140, 1576–1579.
- (32) MacLeod, M. J.; Johnson, J. A. PEGylated N-Heterocyclic Carbene Anchors Designed To Stabilize Gold Nanoparticles in

- Biologically Relevant Media. J. Am. Chem. Soc. 2015, 137, 7974–7977
- (33) Zhang, L.; Wei, Z.; Meng, M.; Ung, G.; He, J. Do polymer ligands block the catalysis of metal nanoparticles? Unexpected importance of binding motifs in improving catalytic activity. *J. Mater. Chem. A* 2020, *8*, 15900–15908.
- (34) Nosratabad, N. A.; Jin, Z.; Du, L.; Thakur, M.; Mattoussi, H. N-Heterocyclic Carbene-Stabilized Gold Nanoparticles: Mono-Versus Multidentate Ligands. *Chem. Mater.* 2021, *33*, 921–933.
- (35) Du, L.; Nosratabad, N. A.; Jin, Z.; Zhang, C.; Wang, S.; Chen, B.; Mattoussi, H. Luminescent Quantum Dots Stabilized by N-Heterocyclic Carbene Polymer Ligands. *J. Am. Chem. Soc.* 2021, *143*, 1873–1884.
- (36) Dominique, N. L.; Chandran, A.; Jensen, I. M.; Jenkins, D. M.; Camden, J. P. Unmasking the Electrochemical Stability of N-Heterocyclic Carbene Monolayers on Gold. *Chem.* ♦ *Eur. J.* 2024, 30, No. e202303681.
- (37) Crudden, C. M.; Horton, J. H.; Narouz, M. R.; Li, Z.; Smith, C. A.; Munro, K.; Baddeley, C. J.; Larrea, C. R.; Drevniok, B.; Thanabalasingam, B.; McLean, A. B.; Zenkina, O. V.; Ebralidze, I. I.; She, Z.; Kraatz, H.-B.; Mosey, N. J.; Saunders, L. N.; Yagi, A. Simple direct formation of self-assembled N-heterocyclic carbene monolayers on gold and their application in biosensing. *Nat. Commun.* 2016, 7, No. 12654.
- (38) Cao, Z.; Derrick, J. S.; Xu, J.; Gao, R.; Gong, M.; Nichols, E. M.; Smith, P. T.; Liu, X.; Wen, X.; Copéret, C.; Chang, C. J. Chelating N-Heterocyclic Carbene Ligands Enable Tuning of Electrocatalytic CO2 Reduction to Formate and Carbon Monoxide: Surface Organometallic Chemistry. *Angew. Chem., Int. Ed.* 2018, *57*, 4981–4985.
- (39) Zhang, L.; Wei, Z.; Thanneeru, S.; Meng, M.; Kruzyk, M.; Ung, G.; Liu, B.; He, J. A Polymer Solution To Prevent Nanoclustering and Improve the Selectivity of Metal Nanoparticles for Electrocatalytic CO2 Reduction. *Angew. Chem., Int. Ed.* 2019, *131*, 15981–15987.
- (40) Rühling, A.; Schaepe, K.; Rakers, L.; Vonhören, B.; Tegeder, P.; Ravoo, B. J.; Glorius, F. Modular Bidentate Hybrid NHC-Thioether Ligands for the Stabilization of Palladium Nanoparticles in Various Solvents. *Angew. Chem., Int. Ed.* 2016, *55*, 5856–5860.
- (41) Rodríguez-Castillo, M.; Laurencin, D.; Tielens, F.; van der Lee, A.; Clément, S.; Guari, Y.; Richeter, S. Reactivity of gold nanoparticles towards N-heterocyclic carbenes. *Dalton Trans.* 2014, *43*, 5978–5982.
- (42) Rodriguez-Castillo, M.; Lugo-Preciado, G.; Laurencin, D.; Tielens, F.; van der Lee, A.; Clement, S.; Guari, Y.; Lopez-de-Luzuriaga, J. M.; Monge, M.; Remacle, F.; Richeter, S. Experimental and Theoretical Study of the Reactivity of Gold Nanoparticles Towards Benzimidazole-2-ylidene Ligands. *Chem. ♦ Eur. J.* 2016, *22*, 10446−10458.
- (43) Arabzadeh Nosratabad, N.; Jin, Z.; Arabzadeh, H.; Chen, B.; Huang, C.; Mattoussi, H. Molar excess of coordinating N-heterocyclic carbene ligands triggers kinetic digestion of gold nanocrystals. *Dalton Trans.* 2024, *53*, 467–483.
- (44) Lei, Z.; Wan, X.-K.; Yuan, S.-F.; Guan, Z.-J.; Wang, Q.-M. Alkynyl Approach toward the Protection of Metal Nanoclusters. *Acc. Chem. Res.* 2018, *51*, 2465–2474.
- (45) Wang, Y.; Wan, X.-K.; Ren, L.; Su, H.; Li, G.; Malola, S.; Lin, S.; Tang, Z.; Häkkinen, H.; Teo, B. K.; Wang, Q.-M.; Zheng, N. Atomically Precise Alkynyl-Protected Metal Nanoclusters as a Model Catalyst: Observation of Promoting Effect of Surface Ligands on Catalysis by Metal Nanoparticles. *J. Am. Chem. Soc.* 2016, *138*, 3278–3281.
- (46) Brown, T. J.; Widenhoefer, R. A. Cationic Gold(I) π -Complexes of Terminal Alkynes and Their Conversion to Dinuclear σ , π -Acetylide Complexes. *Organometallics* 2011, 30, 6003–6009.
- (47) Tang, Q.; Jiang, D.-e. Insights into the PhC \equiv C/Au Interface. *J. Phys. Chem. C* 2015, *119*, 10804-10810.
- (48) Maity, P.; Takano, S.; Yamazoe, S.; Wakabayashi, T.; Tsukuda, T. Binding Motif of Terminal Alkynes on Gold Clusters. *J. Am. Chem. Soc.* 2013, *135*, 9450–9457.

- (49) Wan, X.-K.; Tang, Q.; Yuan, S.-F.; Jiang, D.-e.; Wang, Q.-M. Au19 Nanocluster Featuring a V-Shaped Alkynyl–Gold Motif. *J. Am. Chem. Soc.* 2015, *137*, 652–655.
- (50) Cueto, C.; Hu, W.; Ribbe, A.; Bolduc, K.; Emrick, T. Polystyrene-based Macromolecular Ammonium Halides for Tuning Color and Exchange Kinetics of Perovskite Nanocrystals. *Angew. Chem., Int. Ed.* 2022, *61*, No. e202207126.
- (51) Rahme, K.; Chen, L.; Hobbs, R. G.; Morris, M. A.; O'Driscoll, C.; Holmes, J. D. PEGylated gold nanoparticles: polymer quantification as a function of PEG lengths and nanoparticle dimensions. *RSC Adv.* 2013, *3*, 6085–6094.
- (52) Wang, W.; Wei, Q.-Q.; Wang, J.; Wang, B.-C.; Zhang, S.-h.; Yuan, Z. Role of thiol-containing polyethylene glycol (thiol-PEG) in the modification process of gold nanoparticles (AuNPs): Stabilizer or coagulant? *J. Colloid Interface Sci.* 2013, 404, 223–229.
- (53) Ford, M. J.; Hoft, R. C.; McDonagh, A. Theoretical Study of Ethynylbenzene Adsorption on Au(111) and Implications for a New Class of Self-Assembled Monolayer. *J. Phys. Chem. B* 2005, *109*, 20387–20392.
- (54) Liu, B.; Yao, H.; Song, W.; Jin, L.; Mosa, I. M.; Rusling, J. F.; Suib, S. L.; He, J. Ligand-Free Noble Metal Nanocluster Catalysts on Carbon Supports via "Soft" Nitriding. *J. Am. Chem. Soc.* 2016, *138*, 4718–4721.
- (55) Hu, M.; Jin, L.; Zhu, Y.; Zhang, L.; Lu, X.; Kerns, P.; Su, X.; Cao, S.; Gao, P.; Suib, S. L.; Liu, B.; He, J. Self-limiting growth of ligand-free ultrasmall bimetallic nanoparticles on carbon through under temperature reduction for highly efficient methanol electrooxidation and selective hydrogenation. *Appl. Catal. B: Environ* 2020, 264, No. 118553.
- (56) Bianchini, C.; Shen, P. K. Palladium-Based Electrocatalysts for Alcohol Oxidation in Half Cells and in Direct Alcohol Fuel Cells. *Chem. Rev.* 2009, *109*, 4183–4206.